AN ABSTRACT OF THE THESIS OF

Lu Zheng Meng for the degree of Master of Science in Medical Physics presented on March 14, 2011.

Title: Estimation of the Setup Accuracy of a Surface Image-guided Stereotactic Positioning System.

Abstract approved:

_____

Camille J. Lodwick

Purpose: Stereotactic radiation therapy and stereotactic radiosurgery deliver radiation precisely to tumors, using special equipment to position and demobilize patients. The VisionRT system, with its component AlignRT, is a non-invasive stereotactic positioning and tracking system that uses cameras to capture infra-red images of patients, and process these images, to obtain precise shifts in patient location. This thesis evaluates the accuracy of the AlignRT system accuracy while setting up and tracking patients.

Methods: This thesis investigates the setup accuracy of the AlignRT system based on the CT contour of an anthropomorphic phantom exported to the AlignRT from treatment planning systems, and compared results to those provided by the X-ray image-based positioning system ExacTrac. Measurements

utilize a modified Winston-Lutz technique to derive the deviation of the planned isocenter relative to the radiation isocenter. A phantom embedded with a 16 mm metallic sphere and a Winston-Luts pointer were used as the positioning objects. A Varian electronic portal imaging device were utilized to obtain images. A Vidar scanner and RIT113v5.2 software were used to process images obtained in Winston-Lutz tests. Based on the equations derived for Winston-Lutz tests, shifts of the planned isocenter relative to the radiation isocenter were calculated, which were then used to judge the positioning the objects. Both positioning and tracking modes of AlignRT were tested. AlignRT, ExacTrac, and Winston-Lutz test measurements were all performed on the same Varian Novalis Tx system.

Results: The results indicated that the AlignRT gave a positioning error of more than 1 mm based on CT contours and at small couch angles, which was larger than the clinical tolerance of 1mm for stereotactic radiation therapy. The positioning error would be less if the AlignRT system could be recalibrated with the same isocenter as the X-ray system or utilize its own initial image instead of CT contour. At larger couch angles, the positioning errors were larger than 1 mm even after recalibration. A further investigation and collaboration with the manufacture would be required to obtain desired accuracy.

ESTIMATION OF THE SETUP ACCURACY OF A SURFACE IMAGE-GUIDED STEREOTACTIC POSITIONING SYSTEM

by

Lu Zheng Meng

A THESIS

submitted to

Oregon State University

in partial fulfillment of

the requirements for the

degree of

Master of Science

Presented March 14, 2011

Commencement June 2011

Master of Science thesis of Lu Zheng Meng presented on March 14, 2011

APPROVED:

Major Professor, representing Medical Physics

Head of Department of Nuclear Engineering and Radiation Health Physics

---

Dean of the Graduate School

I understand that my thesis will become part of the permanent collection of Oregon State University libraries. My signature below authorizes release of my thesis to any reader upon request.

Lu Zheng Meng, Author

ACKNOWLEDGEMENTS

I would like to foremost thank Dr. James Tanyi for all the hands-on practices and guidance leading to this research project.

I would like to thank Dr. Camille Lodwick and Dr. Wolfram Laub for their teachings, their role in admitting me to the medical physics program, for serving as adviser, and for granting many privileges for using the facilities at OHSU.

I would like to thank Dr. Ray Hong and Dr. Tony He for introducing me to the field of medical physics.

I would like to thank Mr. Bruce Nimmo who handled my training assistance diligently for the Washington State Workforce Office.

I would like to express my gratitude for Karen Bradley and late Theron M. Bradley, Jr. for supporting me with a scholarship.

Kristie Marsh was the person I turned to every week for signing my never-ending paperwork and I would like to give her a big thank for that and all the other help she provided.

My family's support was unwavering ever since I started on this new career course more than two years ago for which I was truly grateful. My eight-year-old son Phillip was a delight during this period of time as he was also learning terminologies in human anatomy and radiation.

Both Dr. Camille Lodwick and Dr. James Tanyi were extremely helpful for advising me on the contents of the thesis. I would also like to thank Dr. Todd Palmer and Dr. Susan Carozza for serving as my graduate thesis committee members and provide valuable inputs and comments on my thesis. Thanks also goes to Julie Kutz of the Graduate School for checking the format of the thesis.

TABLE OF CONTENTS

Page

Chapter 1. Introduction 1

Chapter 2. Literature Reviews 8

Chapter 3. Material and Methods 11

3.1. Phantom 11

3.2. Treatment Planning Systems 12

3.3. Linac 12

3.4. Film and EPID 13

3.5. Winston-Lutz Test 15

3.6. RIT Software 16

3.7. ExacTrac Measurements of the Winston-Lutz Pointer 17

3.8. ExacTrac Measurements of the Phantom Shifts 22

3.9. AlignRT Isocenter and Calibration 24

3.10. AlignRT Measurement of the Phantom Shifts 25

Chapter 4. Results 39

Chapter 5. Discussion and Conclusion 55

Bibliography 63

LIST OF FIGURES

Figure Page

1. Illustration of the ExacTrac system. A kV X-ray beam is shown to take image of patient cranium for the localization purpose (Illustration by BrainLab). 6

2. ExacTrac and VisionRT Installations at OHSU: (a)ExacTrac infrared detector; (b) ExacTrac X-ray detectors; (c) VisionRT cameras; (d) CBCT; (e) BrainLab couch; (f) Linac. 7

3. Rando phantom with ExacTrac body markers. 28

4. Novalis Tx linac with (a) BrainLab cone and (b)Varian aS500 EPID. 29

5. Depiction of the setup of a cone beam Winston-Lutz test. 30

6. Image taken by EPID in AM Maintenance mode. 31

7. Image as processed by RIT. 32

8. Setup of a Winston-Lutz pointer. 33

9. Coordinate systems used by ExacTrac, VisionRT, Couch, and the EPID. 34

10. Illustration of the projection of the Winston-Lutz pointer on EPID. 35

11. Illustration of the relative distances among the gantry isocenter, ExacTrac isocenter, Winston-Lutz pointer, and the cone centroid. 36

12. AlignRT calibration board at 100 cm SSD. 37

13. User interface of AlignRT module of the VisionRT system. 38

LIST OF TABLES

Table Page

1. Example of the shifts measured from repeated Winston-Lutz tests images of the Winston-Lutz pointer. 48

2. Example of the shifts measured from repeated Winston-Lutz tests images of the phantom. ... 48

3. Comparison of EPID and film. 49

4. Relative shifts of the Winston-Lutz pointer measured by ExacTrac. 49

5. Winston-Lutz test measurements of the Winston-Lutz pointer. 49

6. Offset of the cone relative to the gantry isocenter. 50

7. Offset of pointer relative to gantry isocenter. 50

8. Offsets of ExacTrac isocenter relative to gantry isocenter. 50

9. Wiston-Lutz tests results of the phantom for different gantry and collimator angles. 51

10. Cone offsets calculated from the Winston-Lutz tests of the phantom. 51

11. Offset of the BB relative to gantry calculated from Winston-Lutz measurements of the phantom. 51

12. Offset of the "ExacTrac isocenter" to the gantry isocenter. 52

13. Offsets of the phantom measured by AlignRT after localization by ExacTrac. 52

14. Repeatability of consecutive AlignRT measurements of the same phantom. 53

15. AlignRT measurements of the Rando phantom setup shifts for different body contour CT density cutoff values. 54

16. Testing the consistence of effect of the CT density cutoff for body contour of the phantom on the AlignRT measurement of the setup shifts. 54

17. VisionRT measurements before and after recalibration. 54

Estimation of the Setup Accuracy of a Surface Image-guided Stereotactic Positioning System

Chapter 1. Introduction

This thesis was the result of an ongoing clinical research work done at the Department of Radiation Medicine at Oregon Health and Science University (OHSU) that primarily focused on a new patient positioning system called VisionRT (Vision RT Limited, London, UK). VisionRT is a recently developed non-invasive surface imaging-guided positioning and tracking system that assists in image-guided radiation therapy (IGRT). [1,2,3,4] It is installed in addition to other image-guidance systems for stereotactic radiosurgery (SRS) and stereotactic body radiotherapy (SBRT).

Stereotactic radiosurgery and stereotactic body radiotherapy are intracranial radiation treatment techniques that eradicate tumors with high intensity and high precision radiation, often targeting a small volume in close proximity to sensitive organs or tissues, the so called organs at risk (OARs). Radiation therapy to intracranial lesions is the most common application of these techniques. Due to the large number of radio-sensitive organs in the cranium, SRS/SBRT requires a higher level patient positioning precision compared to

conventional radiation therapy techniques. These requirements construct a good testing environment for the performance of VisionRT.

There are three steps in SRS/SBRT. First is the computed tomography (CT) simulation where the patients undergo virtual simulation using CT scanner. This will generate a series of cross-sectional images of patients from which a 3-D image can be reconstructed for treatment planning. In order to ensure the accuracy of beam delivery in SRS/SRT, the patients typically are immobilized with an immobilization device during the simulation and later during the treatment to prevent the beams overdose healthy tissues and underdose the tumor tissues. Several immobilization devices have been invented in the past for this purpose, including frame-based and frameless devices. Brainlab frame ring is an example of frame-based devices, and thermo-plastic mask frameless. These devices are still widely used.

In the second step, a treatment plan is performed using the CT images. Patient body, OARs, and tumor(s) are contoured using treatment planning algorithms and subsequently used for radiation therapy dose computation. Finally, the treatment plan is exported to the radiotherapy dose delivery system (linear accelerator) for dose administration. Prior to dose administration, the patient is positioned according to setup instructions from the treatment planning system.

Several electronic devices are used to localize the patients before and during the treatment, such as ExacTrac[5] (BrainLAB, Germany), cone-beam computerized tomography[6,7,8] (CBCT) from Varian, electronic portal imaging device [9,10](EPID), and several other ones. At OHSU, ExacTrac, CBCT and EPID are installed in the same treatment room with a Varian Novalis Tx linear accelerator (linac), which provides the capability to improve further the accuracy of localization and treatment of patients.[11]

EXACTRAC

ExacTrac is an automated six-dimensional (6D) patient set-up system that can detect translational and rotational misalignments and provide positional corrections. ExacTrac is fully integrated with the treatment couch, allowing not only accurate set-up verification but also automated patient positioning.

ExacTrac obtains its precise determination of the required correction shift by taking two X-ray images of the patients and comparing them to CT images from treatment planning system. The comparison is based on the bony structures of the patients. The setup of an ExacTrac system is shown in Figure 1.

To track patient location and movement, ExacTrac uses body makers – metallic balls attached to masks or patient's body. The purpose of tracking is mainly to ensure that the patients are localized within preset tolerances.

VISIONRT

The new device under investigation, VisionRT, is meant to serve the same purpose as image-guidance devices such as ExacTrac, in combination with or without immobilization devices. The VisionRT system was installed at OHSU in April 2010 in the same treatment room as. AlignRT is the software component that controls the operation of the VisionRT system. The positioning accuracy of this device was the subject of this thesis. In the remainder of this thesis, the terms VisionRT and AlignRT will be used interchangeably. The ExacTrac system will serve as a reference with which to compare AlignRT system.

AlignRT is a video-based three-dimensional (3D) surface imaging system. Instead of using the anatomic structures of patients to determine the location of patients, AlignRT uses images of skin surfaces of a patient in 3D before and during radiotherapy treatment. The system consists of advanced software, a computer workstation, three 3D camera units, cables, and templates that are used for camera calibration. The system is non-invasive, has the advantage of using infrared light instead of radiation to detect patient positions, and does not require the use of body markers to be put on patients.

AlignRT can acquire images of patient continuously in the tracking mode when it performs as a monitoring and tracking system. In this mode, AlignRT first generates a reference surface of the optimum treatment position determined during treatment simulation. This reference image is generated by either recording

the surface of a patient placed in the treatment room or by importing skin contours from CT volumetric data generated via third party treatment planning software. Prior to each treatment session the patient's position is acquired and compared to the reference image by the system's surface matching software. Where movement or displacement from the reference position is detected, the software calculates new coordinates which can be used to adjust the treatment couch for optimal positioning of the patient.

If deemed precise and easy to use, AlignRT could serve as an additional tool before and/or during the radiation treatment to position and monitor patients. Figure 2 shows the VisionRT system as installed at OHSU.

To study the feasibility of utilizing AlignRT for image-guided radiotherapy, comprehensive testing of positioning and tracking accuracies are necessary. This thesis primarily focused on the accuracy of patient positioning based on the patient's skin CT contour generated from treatment planning systems. While the AlignRT system could utilize its cameras to capture a reference image, such an image does not contain treatment planning information such as the isocenter location, and hence can only used for motion tracking. Therefore, CT-based contoured images were used as reference for the testing of setup accuracy of the AlignRT system.

Figure 1. Illustration of the ExacTrac system. A kV X-ray beam is shown to take image of patient cranium for the localization purpose (Illustration by BrainLab).

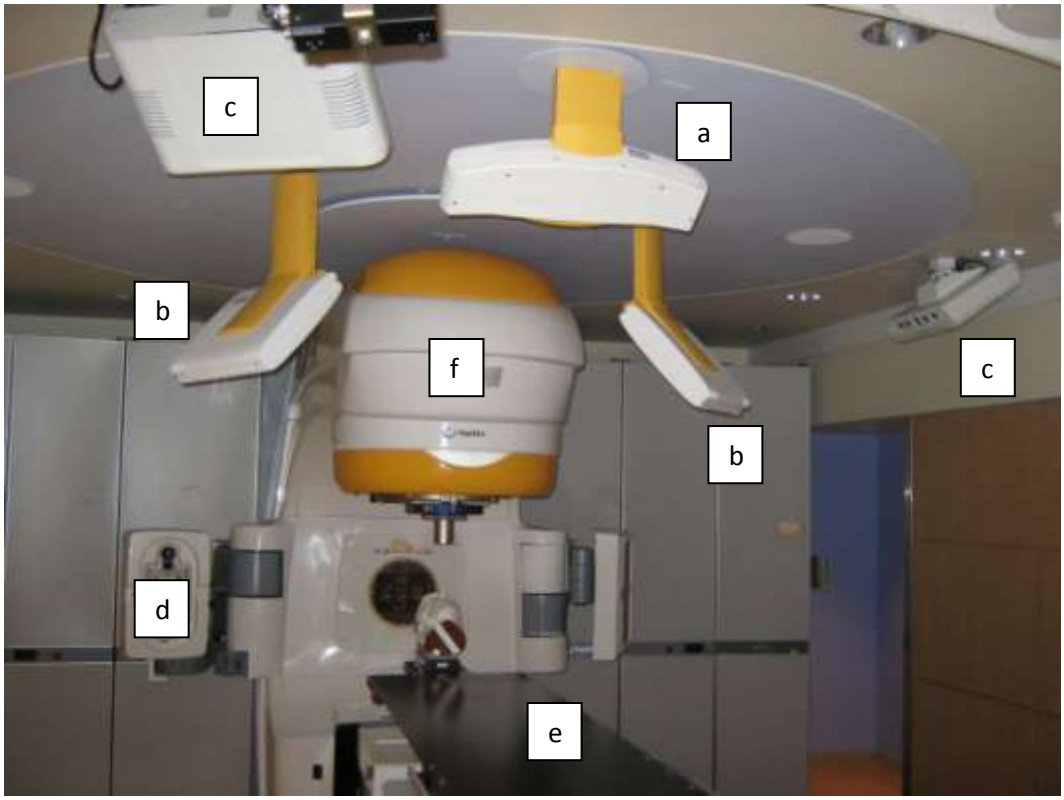

Figure 2. ExacTrac and VisionRT Installations at OHSU: (a)ExacTrac infrared detector; (b) ExacTrac X-ray detectors; (c) VisionRT cameras; (d) CBCT; (e) BrainLab couch; (f) Linac.

Chapter 2. Literature Reviews

Since this thesis addresses specifically the functions of ExacTrac and VisionRT, the articles published by following authors are directly relevant.

Bert *et al.*[3] first introduced AlignRT system and characterized the system as being able to detect and quantify patient shifts in the submillimeter range (0.75 mm) for the three translational degrees of freedom and less than 0.1 degree for each rotation. These shifts, however, were relative movements, and did not indicate the accuracy of localization of patients relative to the radiation isocenter. This thesis research, however, primarily investigated with the shift relative to the radiation isocenter.

Peng *et al.*[12] evaluated the localization accuracy of the AlignRT system and its tracking ability using the CBCT system and an optical tracking system. They used a Rando head-and-neck phantom with a 3mm slice thickness CT images and five real patients, and validated the system accuracy through comparison with the CBCT system of Elekta (Elekta Oncology Systems, Norcross, GA) and the frameless SonArray optical tracking system (Zmed/Varian, Ashland, MA). In this thesis, the phantom used was similar to that used by Peng *et al*., but the slice thickness was 1mm, and the reference system was ExacTrac instead of CBCT.

For the phantom localization study, Peng *et al.* used the optical tracking system to position the phantom isocenter to within 0.1 mm and 0.1° along all three axes. Their results showed that for the origin displacements, the difference between AlignRT and the CBCT systems or between AlignRT and the optical tracking systems was up to 1.3 mm and 1.7°. For phantom displacements having couch angles of 0°, i.e., if no couch rotation was needed, the difference was slightly smaller, at 0.9 mm and 0.4° for CBCT, and 0.3 mm and 0.2° for optical tracking if the references were the previously recorded AlignRT images instead of CT contour surfaces.

For large displacements of more than ±10 mm and ±3°, Peng *et al.* obtained a larger maximum discrepancy between AlignRT and CBCT at 3.0 mm but a smaller discrepancy of 0.4 mm between AlignRT and optical tracking. They further analyzed situation with large couch angles which we tested out in this thesis at 90° and 270° couch angles.

Peng *et al.* also found that the mean registration errors were smaller when using the AlignRT optical surface images than using CT contours, and for patients study, the difference in pretreatment placement was smaller between AlignRT and CBCT than between optical tracking and CBCT.

Peng *et al.* concluded that the AlignRT system could be used for positioning with accuracy comparable to current image/marker-based systems.

Cervina *et al.*[13] examined the feasibility of using AlignRT in a frame-less and mask-less environment and compared the accuracy of AlignRT tracking with that of the optical guidance platform (OGP, Varian Medical Systems, Palo Alto, CA) and showed a difference of 1 mm in displacement and 1° in rotation.

Kim *et al.* [14] compared the accuracy of ExacTrac and CBCT. Although this paper does not relate to AlignRT, the method they used to derive ExacTrac accuracy coincidently bears similarity to the technique utilized in this thesis. This technique was based on the stereotactic radiosurgery system developed by K. R. Winston and W. Lutz[15,16]. Tests using this technique are conveniently called modified Winston-Lutz tests.

To my knowledge, there is no literature that has compared ExacTrac and AlignRT directly, and there are only a couple of institutions that have ExacTrac, AlignRT, and CBCT installations in the same treatment vault. The current work is a phantom-based evaluation of the geometric accuracy and precision of ExacTrac and AlignRT systems on the same clinical radiation therapy delivery system.

Chapter 3. Material and Methods

3.1. Phantom

An anthropomorphic phantom (Rando, The Phantom Laboratory, Salem, NY) was used to study the accuracy of patient setup by AlignRT. Head and neck was the primary area of interest in this study so only the top portion of the phantom was used. This phantom is shown in Figure 3, together with the body markers for ExacTrac.

A 16 mm diameter metal sphere (BB) was inserted into the middle of the phantom to simulate the position of a tumor and served as the location of the treatment plan isocenter. The phantom was scanned by a CT-scanner (Phillips, Andover, MA) with 1-mm slice thickness. A treatment plan was generated using Eclipse 8.4 (Varian Medical Systems, Palo Alto, CA) treatment planning system. The treatment plan isocenter was placed in the center of the BB (later we will see that this was not necessarily to be exact). The plan was then exported to ExacTrac and AlignRT for image-guided localization, so both systems knew where the phantom should be placed according to their own coordinate systems such that the plan isocenter would coincide with the radiation isocenter.

3.2. Treatment Planning Systems

SRS/SBRT treatments at OHSU are planned using iPlan (BrainLAB) or Eclipse treatment planning systems and then delivered on Novalis Tx linear accelerator. The treatment planning for head and neck are mostly done on iPlan system but can also use Eclipse system. In this thesis, the treatment plans were generated from Eclipse system because it provided the interface to both ExacTrac and VisionRT systems.

Since the treatment plan was created with a series of CT scans and the CT scans had a reconstruction resolution of no finer than 1 mm, it needs to be remembered that this uncertainty impacts the position of the plan isocenter, as the center of the BB might not fall on one of the CT slices but be in between slices. The plan isocenter is always chosen to reside on an available CT slice, and when the positioning systems utilizes the plan isocenter to position the phantom, the real center of the BB could be placed slightly off the radiation isocenter.

3.3. Linac

The linac used in this stud was Varian Novalis Tx, equipped with BrainLAB couch table that could move in six degree of freedom. The three translational movements are along the vertical (VRT) or posterior (P)-anterior (A) direction, lateral (LAT) or right(R)-left (L) direction, and longitudinal (LNG) or

inferior (I)-superior (S) direction. The three rotational angles are the couch rotation (RTN) about the vertical axis, the roll about the longitudinal axis (LNG°), and the pitch about the lateral axis (LAT°). This couch has an interface with ExacTrac and can be automatically positioned in six-degree of freedom by ExacTrac. VisionRT does not have interface with the couch and relies on manual adjustment to position the couch along the translational directions.

A BrainLab cone holder fits into the accessory mount on the treatment head of the linac. A 22mm cone was used to collimate the 6MV photon beams in this research.

When the linac gantry rotates around its axis, the intersection of the central radiation beams defines the radiation isocenter which by design should coincide with the gantry isocenter defined by the intersection of the rotational axis of the gantry and the collimator.

3.4. Film and EPID

Once the phantom was positioned into desired location, Winton-Lutz tests were used to acquire near-concentric images of the spherical object and collimated cone beams. By analyzing these images, which will be explained in the General Procedure section, localization accuracy was obtained. Traditional film imaging was initially used in this study. Film has the advantage of providing high resolution images, but takes much longer time to irradiate and process compared

with electronic methods. Films such as Kodak (Rochester, NY) EDR2 radiographic films usually require radiation exposure time of about 200 MUs. Gafchromic films (those that form images without being processed chemically) required 3000 – 5000 MUs of irradiation upon the phantom to get a clear image. Films had to also be scanned by a scanner (Dosimetry Pro Advantage Scanner, Vidar Systems Corporation, Herndon, VA) to obtain images that could be analyzed by software. Since this thesis research required a large number of images to be taken, Electronic portal imaging device (EPID) was sought as a viable tool for capturing images, not only for the current project, but also for future clinical applications. Films were used only as a reference to ensure that the electronic methods delivered the same precision as films.

Varian Novalis Tx is equipped with a Varian aS500 EPID with a resolution of 0.392 mm × 0.392 mm (1,024×768 pixels) on the portal imager. This imager plate is placed by design on the opposite side of the gantry and controlled remotely, as shown in Figure 4. The further away the plate is from the isocenter, the higher its resolution. The source to the detector distance used in this study ranged from 135 to 150 cm, translating to a resolution of 0.26 to 0.29 mm at the isocenter.

EPID is designed to take real-time image while patients are treated and can operated using several modes. One mode is for maintenance purpose called ‘AM Maintenance’. This mode was utilized to obtain images in this study because

it required a very small amount of irradiation to form an image. Most images only needed a few MUs, a great speedup over films. In most cases, three images were taken for every instance to ensure that at least one of them could be analyzed automatically. When all three were read, an average of the readings was taken to give better accuracy.

3.5. Winston-Lutz Test

Winston-Lutz test refers to a setup where a square or cone beam from the gantry irradiates at a spherical target and several images are taken with different gantry angles on a film at the opposite side of the gantry. It serves as stereotactic radiosurgery QA test, but it can also be used as a quantitative method to determine setup accuracy. The setup for Winston-Lutz test is shown in

Figure **5**. Modifications are usually made to the Winston-Lutz tests depending on their purpose. In this thesis, the modified Winston-Lutz tests acquired pairs of images with the beams set at opposing gantry or collimator angles. An example of a Winston-Lutz test image taken by the AM Maintenance mode of the control console is shown in Figure 6.

Throughout the experiments, a 22 mm cone was used to collimate the beam as it was slightly larger than the 16 mm BB inside the phantom, but was not too large in comparison to the 5 mm sphere inside the Winston-Lutz pointer.

3.6. RIT Software

Both films scanned by Vidar scanner and EPID images are processed by RIT113 (Version 5.2, Radiological Imaging Technology, Colorado Springs, CO). During the processing, calibration and sometimes filtering needed to be applied to the images. RIT113 software (RIT) has a stereotactic cone concentricity function that calculates the distance of the central circle relative to the center of the outer circle and breaks it down into shifts along the lateral as X-direction and along the longitudinal as Y-direction, as shown in Figure 7. If the X-shift is positive, the inner circle is more to the right (left side of the couch) of the outer circle when looking down, and Y-shift is positive when the inner circle is more towards inferior (away from the gantry) than the outer circle. Using RIT to evaluate measurements requires several parameters to be input into the software, because RIT software is independent from the treatment system and does not obtain the setup distances between the object and its projected image on EPID. Therefore, in order to process stereotactic cone alignment, the following information was put into the software:

- Size of the area
- Size of the cone on the image
- Magnification factor

- Number of images to be analyzed

When Vidar scanner was used to scan films, its resolution was set at 300 dpi which corresponded to 0.08 mm. Images obtained by EPID had a resolution of 0.26 mm.

3.7. ExacTrac Measurements of the Winston-Lutz Pointer

Like all the positioning systems used in the clinic, ExacTrac and room lasers were calibrated and checked periodically. Ideally, the ExacTrac isocenter, the intersection of the laser beams, and the gantry isocenter coincide in space. When ExacTrac system is well aligned with laser beams and gantry isocenter, the spatial separation between the ExacTrac isocenter and the gantry isocenter is quite small, in the submillimeter range. To ensure that the ExacTrac isocenter stays in the proximity of the gantry isocenter, calibrations of the ExacTrac were carried out periodically by the medical physicist staff. This procedure takes two steps. The first step is to identify the isocenter. A simple way to do this is to attach the 1- meter pointer stick to the gantry and verify that the laser beams meet at the tip of the stick pointer with the gantry at different angles. The intersection of all the laser beams is then the gantry isocenter. In the second step, align the ExacTrac phantom to the gantry isocenter, and let the ExacTrac system detect the phantom and remember the spatial location of the isocenter. This defines ExacTrac's own isocenter. The deviation of the ExacTrac isocenter relative to the gantry isocenter

is an important indicator of how well the ExacTrac system is calibrated and maintained.

An accessory of the ExacTrac system called the Winston-Lutz pointer as shown in Figure 8 is used to measure the localization of the ExacTrac system, i.e., the relative position of the pointer to the ExacTrac system and the relative position of the ExacTrac system to the gantry system. ExacTrac provides a calibration function that measures the shift of the Winston-Lutz pointer relative to the ExacTrac isocenter once the pointer is positioned close to the gantry isocenter as aligned by laser beams. These measurements would provide the systematic error for the ExacTrac system relative to the radiation isocenter. Since the flat panel detectors of the ExacTrac system are 20 cm by 20 cm in size and 512 × 512 pixels, it translates to an image resolution of 0.4 mm × 0.4 mm at the isocenter. The following notations are used to denote the relative shift of the Winston-Lutz pointer to the ExacTrac isocenter. Figure 9 shows the coordinate systems used by ExacTrac, AlignRT, couch, and portal imager.

VRT_{exa}^{ptr} : Vertical shift of the Winston-Lutz pointer relative to the ExacTrac isocenter, positive in anterior direction (A/+)

LNG_{exa}^{ptr} : Longitudinal shift of the Winston-Lutz pointer relative to the ExacTrac isocenter, positive in superior direction (S/+)

LAT_{exa}^{ptr} : Lateral shift of the Winston-Lutz pointer relative to the ExacTrac isocenter, positive in left direction (L/+)

After the shifts are measured, portal images of the Winston-Lutz pointer are acquired with the EPID and the resulting images are analyzed with RIT. Let the following notations denote the shifts given by RIT.

$S_{X,ptr}^{\theta,\varphi}$: Shift of the pointer centroid relative to the cone centroid projected in the lateral direction on EPID with the linac at θ-degree gantry angle and φ-degree collimator angle.

$S_{Y,ptr}^{\theta,\varphi}$: Shift of the pointer centroid relative to the cone centroid projected in the longitudinal direction on EPID with the linac at θ-degree gantry angle and φ-degree collimator angle.

A Winston-Lutz test consists of a pair of images taken at the opposite beam angles. Gantry angles of 90° and 270° are paired up, and collimator angles of 90° and 270° are also paired up. Figure 10 shows the projection of an image viewed from the gantry when the gantry is at 90°. As shown in Figure 11, the shifts from the opposite gantry angles let one calculate the pointer offset relative to gantry isocenter in the vertical direction, VRT_{g}^{ptr}, as

$$VRT_g^{ptr} = \frac{S_{X,ptr}^{90,\varphi} - S_{X,ptr}^{270,\varphi}}{2} \quad (1).$$

VRT_g^{ptr} is positive in the anterior (A/+) direction and the collimator angle φ are chosen to be 90° and 270°. At the same time, the vertical shift of the cone can also be calculated. However, when the gantry is at 90° or 270°, what appears to be vertical shift for the cone is actually the lateral shift of the cone relative to the gantry, LAT_g^{cone}, expressed as

$$LAT_g^{cone} = \frac{S_{X,ptr}^{90,\varphi} + S_{X,ptr}^{270,\varphi}}{2} \quad (2).$$

One can see that the vertical shift of the pointer can be calculated solely from the shifts measured from the EPID images. Even if the cone were not positioned exactly in the center of the gantry, the relative distance from the pointer to the gantry isocenter could still be found. In case the beams from the gantry at 90° and 270° did not coincide, the average of the beam location would be considered as the gantry isocenter, and above equations would give the shifts relative to the average isocenter.

Using the above technique, one could also find the lateral and longitudinal shifts of the pointer and cone relative to the gantry isocenter. This time, the shifts are calculated not from the gantry rotations but from the collimator rotations. The gantry is still rotated to give multiple results for comparison. The X-shifts at

collimator angle of 90° and 270° and gantry angle of 0° give the lateral offset as follows

$$LAT_g^{ptr} = \frac{S_{X,ptr}^{0,90} + S_{X,ptr}^{0,270}}{2} \quad (3).$$

$$LAT_g^{cone} = \frac{S_{X,ptr}^{0,90} - S_{X,ptr}^{0,270}}{2} \quad (4).$$

with the positive direction for lateral shift pointing to the left (L/+). The longitudinal shifts are obtained from the Y-shifts

$$LNG_g^{ptr} = \frac{S_{Y,ptr}^{\theta,90} + S_{Y,ptr}^{\theta,270}}{2} \quad (5).$$

$$LNG_g^{cone} = \frac{S_{Y,ptr}^{\theta,90} - S_{Y,ptr}^{\theta,270}}{2} \quad (6).$$

with the positive direction to the inferior (I/+), i.e., away from the gantry, and gantry angle θ taking values of 0°, 90°, and 270°.

Since the relative distance from the pointer to the gantry isocenter is calculated by Eqs. (1, 3, 6), and the distance from the pointer to the ExacTrac isocenter is given by ExacTrac, the distance from the ExacTrac isocenter to the gantry isocenter can also be calculated. These are

$$VRT_g^{exa} = VRT_g^{ptr} - VRT_{exa}^{ptr} \quad (7).$$

$$LAT_g^{exa} = LAT_g^{ptr} + LAT_{exa}^{ptr} \quad (8).$$

$$LNG_g^{exa} = LNG_g^{ptr} + LNG_{exa}^{ptr} \quad (9).$$

The plus sign in the lateral and longitudinal distance calculation is due to the different coordinate systems used by ExacTrac and the EPID.

3.8. ExacTrac Measurements of the Phantom Shifts

The phantom is measured in the same way as the Winston-Lutz pointer in the sense that the BB inside the phantom acts the same as the sphere inside the Winston-Lutz pointer and that the computation used for the Winston-Lutz pointer, Eq. (1-6), could also be used for the phantom. Similar notations were used for phantom, with "ball" as the subscript.

$S_{X,ball}^{\theta,\varphi}$: Shift of the ball centroid relative to the cone centroid projected in the lateral direction on EPID with the linac at θ-degree gantry angle and φ-degree collimator angle.

.

$S_{Y,ball}^{\theta,\varphi}$: Shift of the ball centroid relative to the cone centroid projected in the longitudinal direction on EPID with the linac at θ-degree gantry angle and φ-degree collimator angle.

$$VRT_g^{ball} = \frac{S_{X,ball}^{90,\varphi} - S_{X,ball}^{270,\varphi}}{2} \quad (10).$$

$$LAT_g^{cone} = \frac{S_{X,ball}^{90,\varphi} + S_{X,ball}^{270,\varphi}}{2} \quad (11).$$

$$LAT_g^{ball} = \frac{S_{X,ball}^{0,90} + S_{X,ball}^{0,270}}{2} \quad (12).$$

$$LAT_g^{cone} = \frac{S_{X,ball}^{0,90} - S_{X,ball}^{0,270}}{2} \quad (13).$$

$$LNG_g^{ball} = \frac{S_{Y,ball}^{\theta,90} + S_{Y,ball}^{\theta,270}}{2} \quad (14).$$

$$LNG_g^{cone} = \frac{S_{Y,ball}^{\theta,90} - S_{Y,ball}^{\theta,270}}{2} \quad (15).$$

The directions of the shifts take the same sign as those for the pointer. Notice that the shift of the cone relative to the gantry is calculated once more, this time using the images from the BB inside the phantom. This can be compared to the shifts calculated from Winston-Lutz pointer and serves as a consistency check between the pointer and the phantom. Ideally, there should be no difference.

Similar to Eqs. (7, 8, 9), the distances between the ExacTrac isocenter and the gantry isocenter can be extracted from the measurements on the phantom in the same way as from the Winston-Lutz pointer.

$$VRT_g^{exa} = VRT_g^{ball} - VRT_{exa}^{ball} \quad (16).$$

$$LAT_g^{exa} = LAT_g^{ball} + LAT_{exa}^{ball} \quad (17).$$

$$LNG_g^{exa} = LNG_g^{ball} + LNG_{exa}^{ball} \quad (18).$$

As will be noted in Chapter 5, there is a difference in the shifts of the ExacTrac isocenter relative to the gantry isocenter between that calculated from the measurements of the Winston-Lutz pointer and that calculated from the phantom measurements. In both cases, these calculation give the estimates of how accurate the ExacTrac system is aligned with the gantry system.

3.9. AlignRT Isocenter and Calibration

To make the shifts from ExacTrac and AlignRT systems comparable, it is useful to look at how AlignRT defines its isocenter. AlignRT assumes its own isocenter based on its calibration. For the calibration, a dotted board is used (c.f. Figure 12). According to AlignRT User Guide 1.0, the board should be put at exactly the gantry isocenter location for calibration. SSD light and the 1-meter stick pointer are used to position the board. In this way, the board is precisely set at 100 cm, which is the designated isocenter location of the gantry by design. Furthermore, the board also is set to be horizontal, and its own cross lines

matched the gantry crosshair and the laser beams. Since the laser beams match the tips of the pointer in all axes, once the center of the board is matched with the pointer and the cross lines of the board matched with the laser beams, it can be assumed that the center of the board is also the isocenter of the gantry. Therefore, this center serves as the isocenter of the AlignRT.

AlignRT needs to be calibrated regularly. A daily calibration is required most of the time, which takes into account the possible movement from cameras and sensors. A monthly calibration, which decides the isocenter location, is needed from time to time when daily calibration fails. At the end of daily calibration, AlignRT provides two root-mean-square (RMS) readings of all the dots on the board. If these RMSs were large, e.g. close to 1 mm, the calibration then would fail. AlignRT then prompts the users to perform a new monthly calibration.

3.10. AlignRT Measurement of the Phantom Shifts

AlignRT determines the shifts of the phantom along the vertical, longitudinal, and lateral directions where they should be applied to the phantom in order for the phantom plan isocenter to be positioned at the radiation isocenter. After the phantom is positioned using ExacTrac system, the same CT contour used in ExacTrac is also imported into AlignRT. AlignRT then uses this image as the reference and compared them to the instantaneous images that its cameras

acquire of the phantom. Based on its algorithms, AlignRT calculates the shifts needed to move the phantom into the correct position. These shifts are reported as

ΔVRT: Vertical shift, positive in the anterior direction

ΔLNG: Longitudinal shift, positive in the superior direction

ΔLAT: Lateral shift, positive in the left direction

ΔLNG°: Rotational shift about the longitudinal axis, a.k.a. roll.

ΔLAT°: rotational shift about the lateral axis, a.k.a. pitch.

ΔRTN: rotational shift of the couch angle.

Even though AlignRT could calculate the translational and rotational shifts needed to position the phantom to be at the isocenter according to AlignRT, there is no interface between AlignRT and the couch. Shifts can only be manually applied via the Varian console and only the translational shifts and couch rotation can be applied.

AlignRT uses a user-defined area of the patient as the region of interest (ROI), as shown in Figure 13. AlignRT's algorithm then uses this area to compute the localization shifts. This ROI is user defined and can take shapes of a contoured area. The default ROI covers an area that encompasses the entire phantom. Smaller ROIs were experimented, as were ways to determine if the

sizes of the ROI gave better resolution for localization. The smaller the ROI, the faster the computation would be.

When the phantom is ready to be measured, AlignRT beams infrared light onto the phantom and its cameras acquire images, after which AlignRT performs evaluation of the images where it compares the images with the CT contour and calculates the shifts.

Figure 3. Rando phantom with ExacTrac body markers.

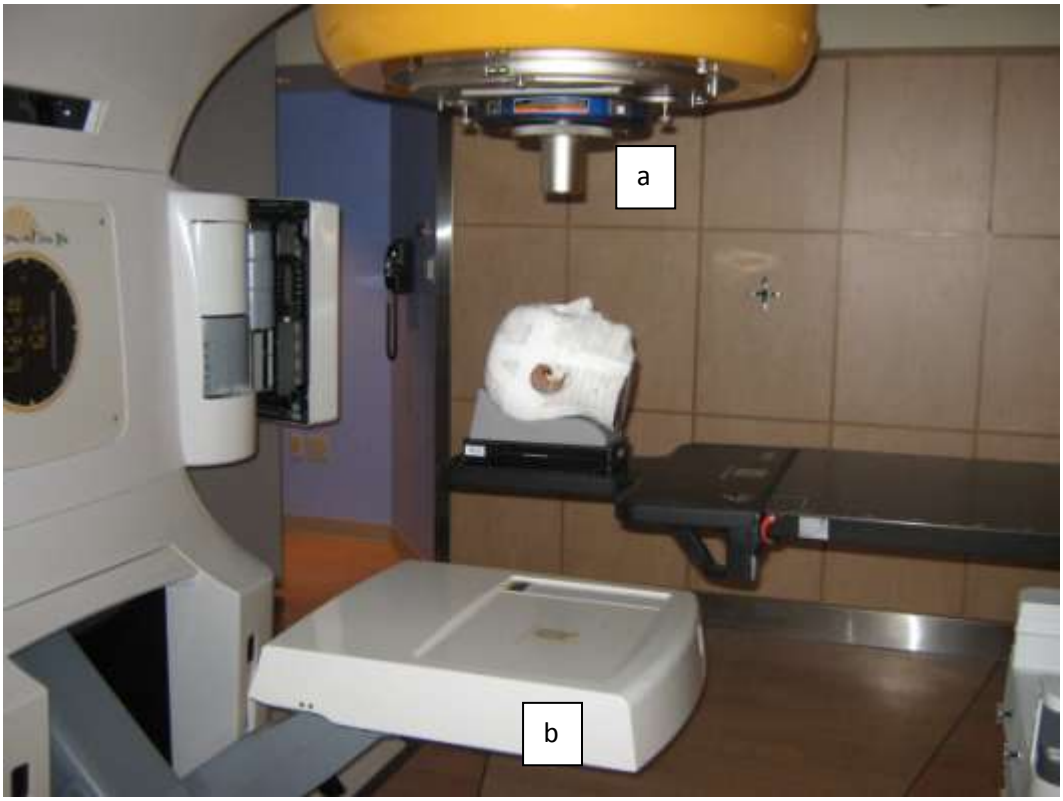

Figure 4. Novalis Tx linac with (a) BrainLab cone and (b)Varian aS500 EPID.

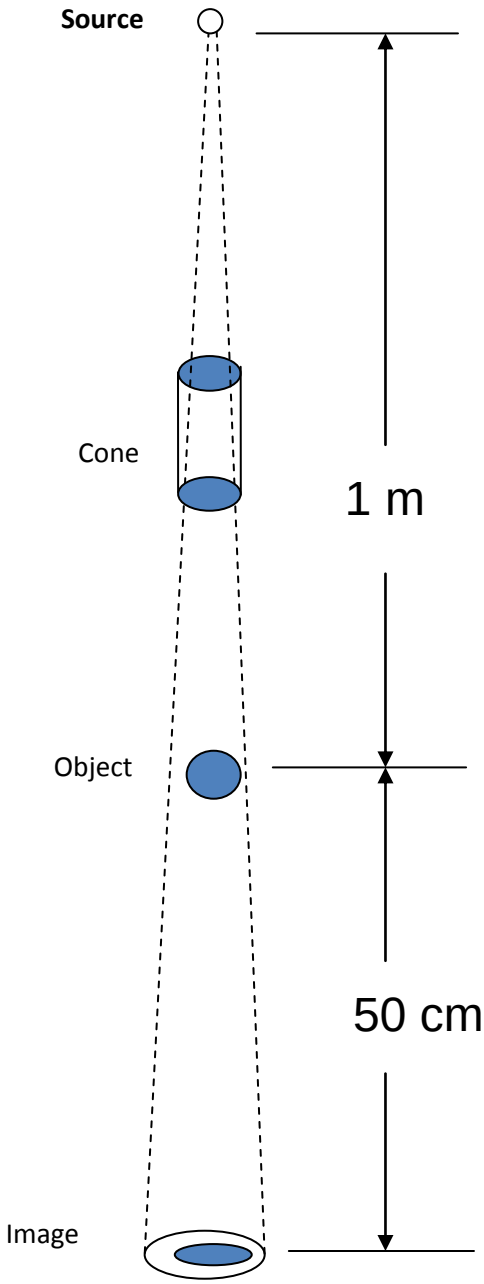

Figure 5. Depiction of the setup of a cone beam Winston-Lutz test.

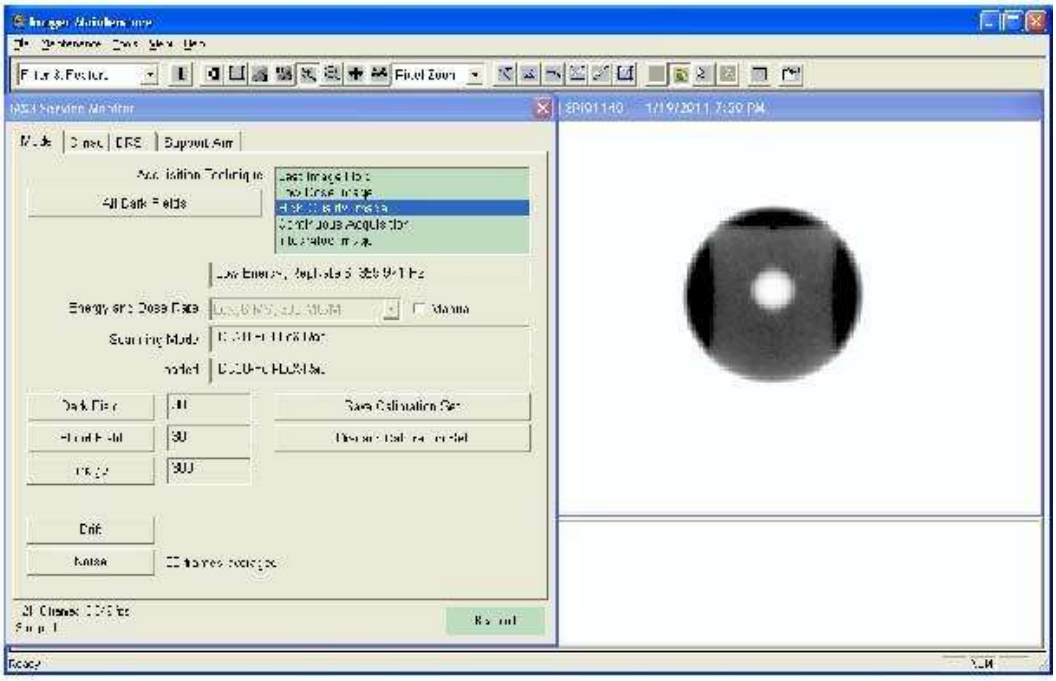

Figure 6. Image taken by EPID in AM Maintenance mode.

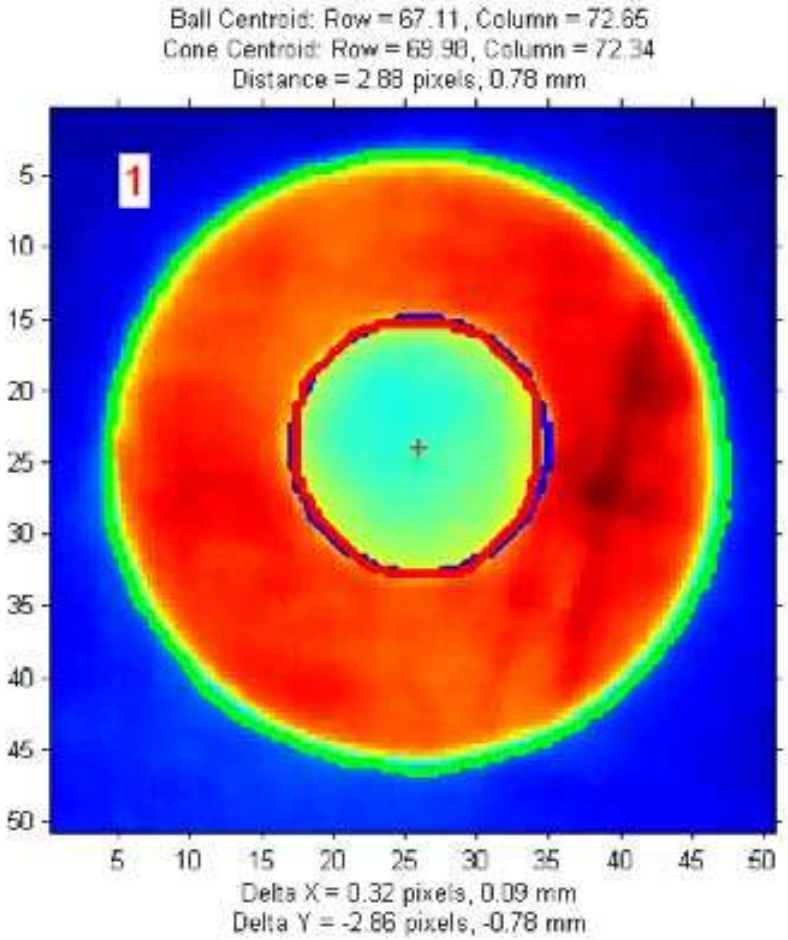

Figure 7. Image as processed by RIT.

Figure 8. Setup of a Winston-Lutz pointer.

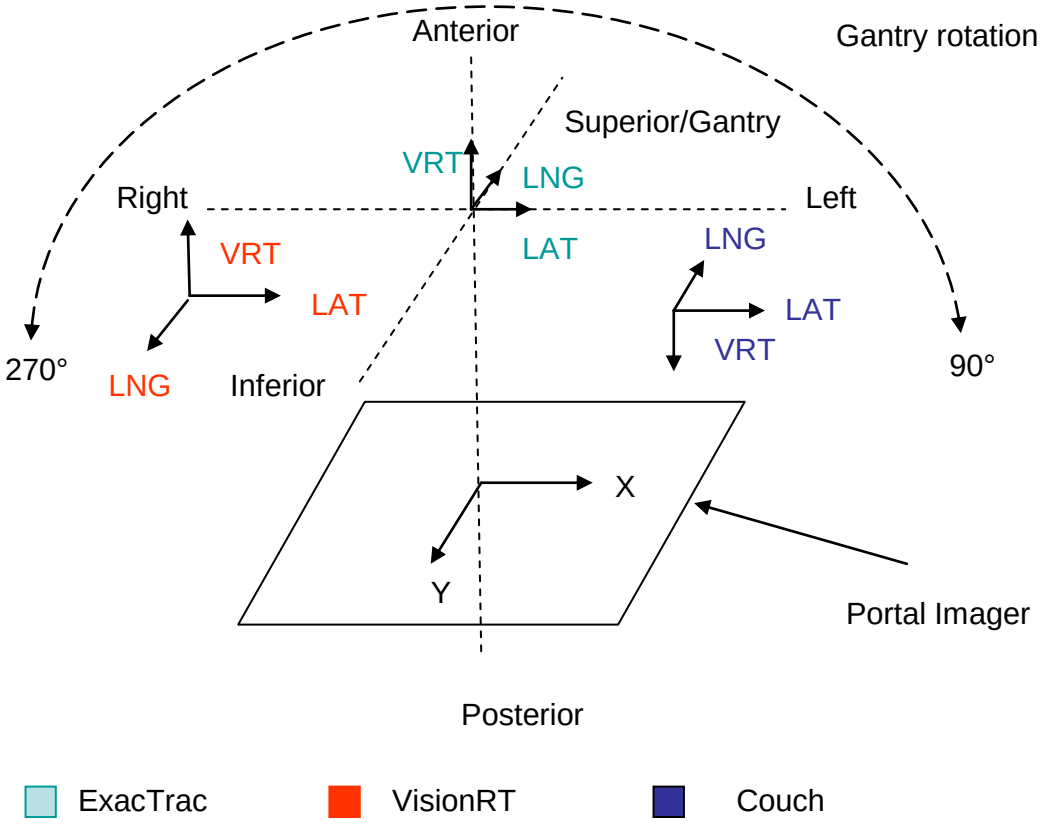

Figure 9. Coordinate systems used by ExacTrac, VisionRT, Couch, and the EPID.

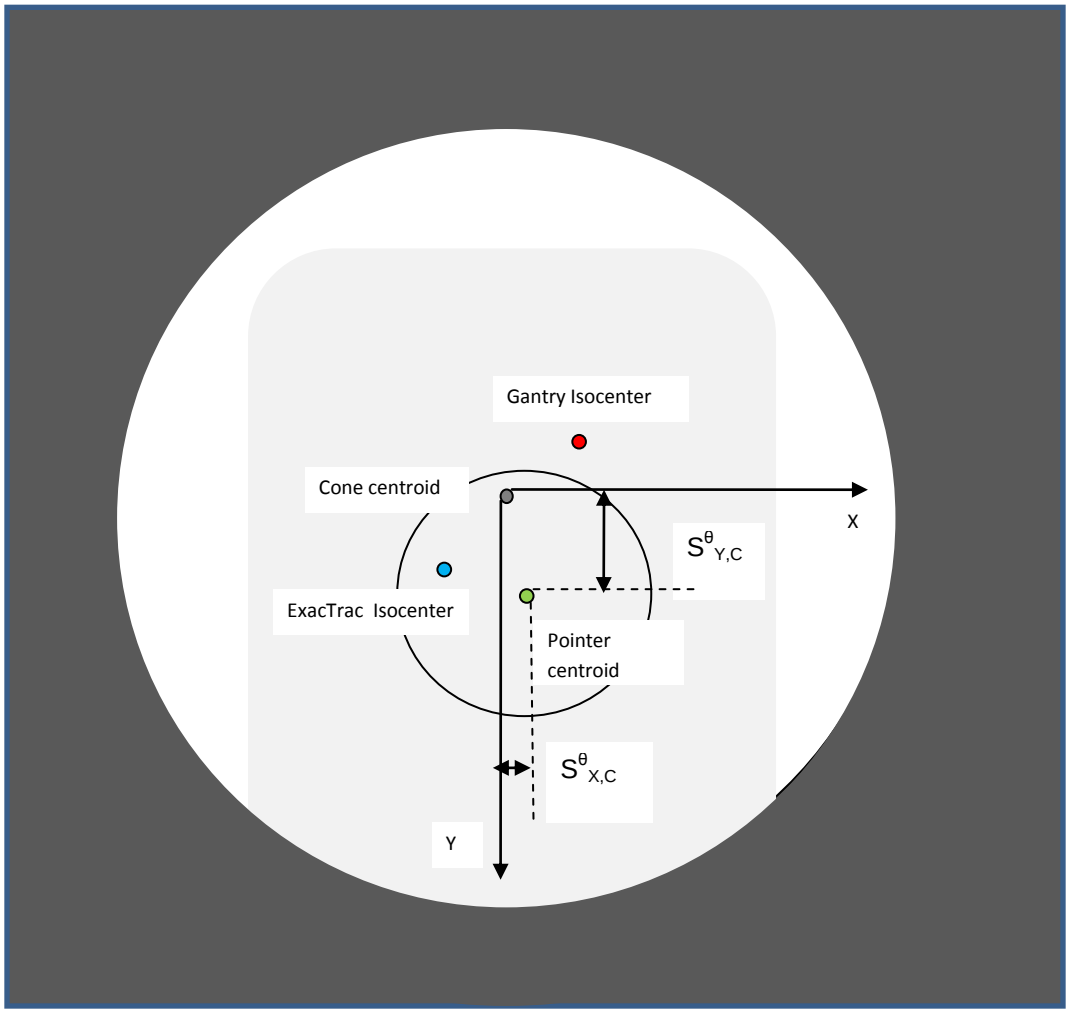

Figure 10. Illustration of the projection of the Winston-Lutz pointer on EPID.

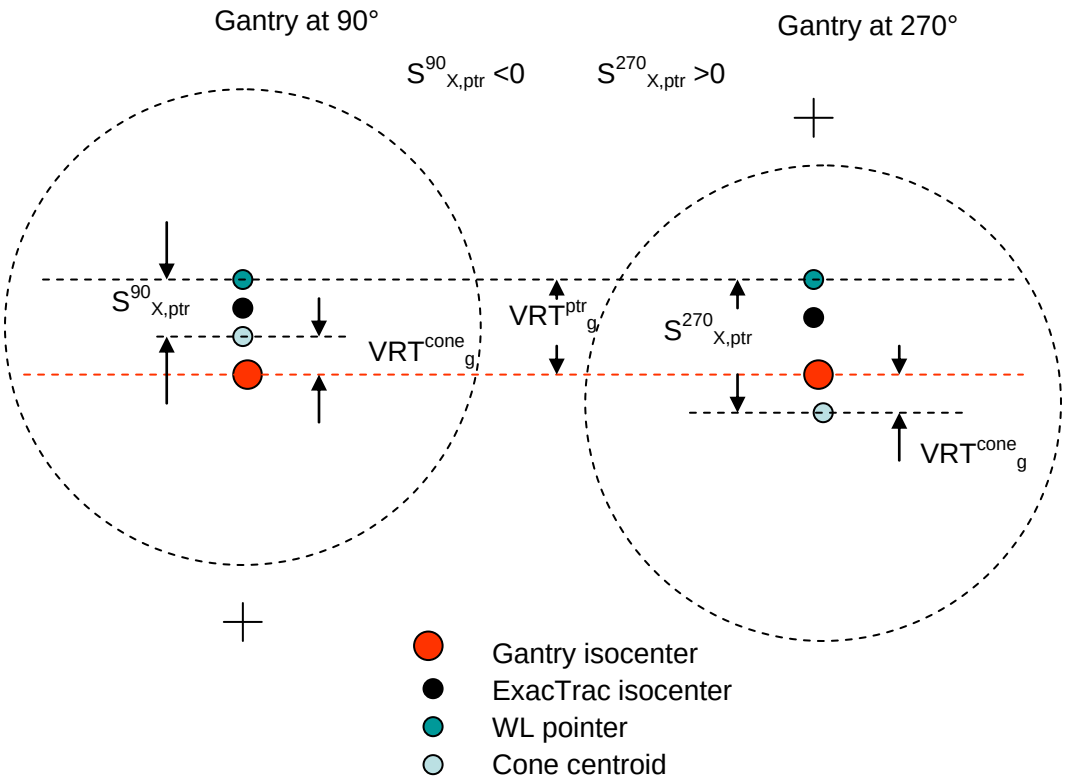

Figure 11. Illustration of the relative distances among the gantry isocenter, ExacTrac isocenter, Winston-Lutz pointer, and the cone centroid.

Figure 12. AlignRT calibration board at 100 cm SSD.

Figure 13. User interface of AlignRT module of the VisionRT system.

Chapter 4. Results

During the period that this study was conducted, it was verified that the positions of the 1-meter pointer stick at 0°, 90°, 180°, and 270° gantry angles were always aligned with the gantry rotation axes. Observing the positions of the 1-meter pointer stick at different gantry angles gave an indication of where the gantry isocenter was located. At different gantry angles, the intersection of the laser beams and the pointer tip showed the position of the isocenter. It was observed that the pointer was confined to a volume of less than 1 mm^3 at the tip of the pointer during the gantry rotation. At 0° and 180° gantry angles, the tip of the pointer was within laser beams from left and right, and at 90° and 270°, it was also within the laser beams from the top. Therefore, it could be stated that the laser beams were aligned with gantry rotations and that the pointer stick could also serve for the calibration of the AlignRT system.

As mentioned in Chapter 1, the EPID was tested in this research as a viable tool for capturing images. Several tests were carried out to check the repeatability of the measurements.

Table 1 shows the measurements of ten consecutive EPID images of the stationary Winston-Lutz pointer, as analyzed and calculated by RIT. The maximum deviation of the data set showed that repeated images of the Winston-Lutz pointer differed very slightly. Repeated imaging of the phantom also showed

similarly narrow spread among consecutive images, as indicated in Table 2. Since the evaluation of the images by RIT appears to be consistent from one measurement to the next, it is reasonable to take the maximum deviation of 0.05 mm as the measurement error, which can be ignored when compared to the resolution of the EPID of 0.26 mm.

Table 3 compares images taken by EPID and Kodak EDR2 film of the same stationary Winston-Lutz pointer. The difference in the shift measured by EPID and Film was in the neighborhood of 0.1 mm. The error on the measurements was the combination of the scanner resolution of 0.08 mm and the EPID resolution of 0.26 mm. The small difference between the film and EPID justified the decision to replace films with EPID for this research.

All of the following measurements were performed on the same day (Jan 18th, 2011) to ensure that the ExacTrac and AlignRT both measured the same setup. The same tests were repeated the next day and the results were similar. More measurements were also carried out over a period of three weeks to confirm different aspects of the procedure, leading to the final round of conclusive experiments as presented here.

The Winston-Lutz pointer was positioned and aligned with lasers. Table 4 shows the relative positions of the Winston-Lutz pointer to the ExacTrac isocenter, as given by the calibration function of ExacTrac. Afterwards, EPID images were taken at 0°, 90°, and 270° gantry angles and 90° and 270° collimator

angels. To process the images using RIT, the size of the projected area of the cone beam was usually put at 4 or 5 cm. Size of the ball on the image was put between 1.6 cm and 2 cm for the BB inside the phantom or .5 cm for ball inside the Winston-Lutz pointer. Magnification factor is the ratio of SSD to source-EPID-distance or source to film distance. EPID was set either at 135 cm or 150 cm from the source, and film was set on top of EPID which was 146.7 cm. These correspond to a magnification factor of 0.74, 0.66, and 0.68, respectively. RIT uses the magnification factor to calculate the displacement and provide an estimate of the size of the object based on the images, which should reflect the sizes of the objects (16 mm for BB or 5 mm for pointer).

The distances between concentric circles on the EPID images of the Winston-Lutz pointer were measured by RIT and shown in Table 5. Even though the cone had a wiggle room of 0.75 mm, the cone was shown to be set very close to the gantry center, Table 6, with an error of ±0.18mm based on the resolution of the EPID. Offsets of the pointer relative to the gantry isocenter were then calculated with Eqs. (1,3,6) as shown in Table 7. Repeated measurements of the Winston-Lutz pointer by the calibration function (not shown) provided an error range of ±0.2mm, therefore the error on the offset of the pointer relative to the gantry isocenter was ±0.27 mm. This offset result shows that the shift of the pointer relative to the gantry isocenter was extremely small when the pointer was aligned with the lasers. These could be coincidental, as the relative distance

between the ExacTrac isocenter and the gantry isocenter could be even larger than these (see next paragraph). Notice that the longitudinal shifts as calculated from measurements at 90° and 270° gantry angles were slightly larger than that at 0°. This was probably due to the gantry sag at 90° and 270°. This effect did not show up on the calculation for the cone offset because the cone was fastened on the gantry head and moved together with the gantry.

Based on the above results, the distance from the ExacTrac isocenter to the gantry isocenter was calculated using Eqs. (7, 8, 9) and shown in Table 8, with an error of ±0.32 mm. These offsets of the ExacTrac isocenter to the gantry isocenter were still small even though they were larger than those between the pointer and the gantry isocenter in vertical direction. Again, the longitudinal shift results for 90° and 270° gantry angles were slightly larger than that at 0°, probably due to gantry sag. Repeated measurements confirmed that these results were reproducible. Based on these results, it could be concluded that the ExacTrac and the laser beams were considered well aligned and the ExacTrac isocenter and gantry isocenter were also aligned.

After the pointer position was measured, the phantom was placed on the couch and localized by ExacTrac. On the Varian console, the couch positions were 16.3, 48.5, 998.6, and 0.4° for VRT, LNG, LAT and RTN respectively. From the EPID images taken at 0°, 90°, and 270° gantry angles and 90° and 270° collimator angels, distances between concentric circles projected by the BB inside

the phantom and the cone were measured by RIT and shown in Table 9, from which the lateral and longitudinal offsets of the cone relative to the gantry center were each calculated in three different ways using Eqs. (11, 13, 15) and shown in Table 10.

These numbers were consistent with those from Table 6 in both the sign and magnitude, within the range of error of ±0.18mm, because these were the shifts of the same cone that did not move relative to the gantry. Calculated offsets of the BB relative to the gantry isocenter using Eqs. (10, 12,14) are shown in Table 11. These results were also similar to but not the same as those obtained from Winston-Lutz pointer. Nonetheless, the BB was positioned very close to the gantry isocenter. Notice that the longitudinal shifts again appeared to be larger when measured at gantry angles 90° or 270°, probably due to the gantry sag.

While the Winston-Lutz pointer was aligned manually with the laser beams, the phantom and thus the BB inside it were aligned by ExacTrac based on the CT contours. The above results were an indication that the ExacTrac indeed placed the object accurately at the intended location.

After ExacTrac placed the object and went through the positioning process, it verified the distance between the isocenter of the phantom and the ExacTrac isocenter. For the phantom setup here, the verification indicated the shifts as VRT_{exa}^{ball} = -0.13 mm, LNG_{exa}^{ball} = 0.10 mm, LAT_{exa}^{ball} = 0.02 mm for

VRT(A/+), LNG(S/+), and LAT(L/+) direction and 0.1°, 0.0°, 0.1° for rotation (RTN), roll (LNG°), and pitch (LAT°). With this information, the offset between the ExacTrac isocenter and the gantry isocenter could be calculated by Eqs. (16, 17, 18). The result is shown in Table 12.

These results for the ExacTrac isocenter were different from those obtained for the Winston-Lutz pointer shown in Table 8. Except for the longitudinal shift, both vertical and longitudinal shifts differed by around 0.6 mm between the two. As will be discussed later, this could likely be traced back to the accuracy of the placement of the isocenter in the CT contour of the phantom. If the plan isocenter were slightly off the center of the ball due to the slice thickness of the CT image, the ExacTrac's placement of the center of the BB would result in a slight shift from the center of the beam which would show up on the EPID images. The difference between the ExacTrac isocenter in Table 8 and Table 12 is a measure of how much off the phantom isocenter is from the center of the BB. This does not apply to the Winston-Lutz pointer because it did not involve contouring the object.

With the phantom still in the same location, AlignRT was used to measure the shifts. These shifts let the users know how far the phantom should be moved in order to be at the same location as indicated by the treatment plan. The results are shown in Table 13.

.

Notice that the translational offsets are expressed in centimeters. If these numbers were correct, the phantom had to be shifted significantly out of the location set by ExacTrac. ExacTrac would give a warning that the object was out of range. Earlier it was mentioned that the AlignRT system was a 3D system and implied that only the translational shifts could be applied. Rotational shifts could in principle be applied as well, but that would require the AlignRT reexamine the phantom and consequently produce another set of offset measurement. Additional offset measurements would further lead to another round of movement until eventually all the offset were within an acceptable range. In clinical practice, this type of iteration would be too time-consuming unless AlignRT had the capability to directly control the couch. So for now, only the translational shifts were considered Table 13 indicated a large shift beyond the tolerance of SRS/SBRT.

To ensure that the AlignRT measurements were consistent, repeated readings were taken on a stationary phantom. A list of the shifts evaluated repeatedly by AlignRT is shown in Table 14. The maximum deviation of 0.1mm implies that one to three evaluations by AlignRT should be sufficient provide accurate reading of each position of the phantom.

Since AlignRT obtains measurements based on the surface, and the surface dimensions of the reference images created by CT images are partially affected by the contours of the reference body in the treatment planning systems, measurements were performed to investigate how different contours affect the

AlignRT measurements. These contours were chosen based on the cutoff Hounsfield units used in the automatic "Search Body" function of the Eclipse treatment planning system. Different cutoff units would produce different contours, with higher Hounsfield unit resulting in smaller contour and lower Hounsfield unit resulting in larger contour.

To investigate how cutoff units affected AlignRT measurements, contours created with different Hounsfield units for the phantom were exported to the AlignRT system with cutoff ranging from -100 to -900 HU, i.e., from close to water to almost air. Most treatment plan used a default cutoff unit number, such as -350 HU assigned to the body in order to automatically create the contour of the body. Tissues that were below -350 HU were considered as part of the body, and those above this cutoff number were outside the body. By assigning different cutoff values to the body, the contours were slightly tighter or loser, reflecting the inclusion or exclusion of the surface material such as mask or tapes. When using these contours as reference image in AlignRT, the results measurements of the shifts greatly differed. The results are shown in Table 15 and Table 16 for the phantom measured on two separate days.

RECALIBRATION

The AlignRT system is currently still evolving, with newer versions of the software rolling out in the coming months. One of the capabilities would allow the user to define isocenter manually. For example, in this study, the phantom was

perceived to be positioned accurately by ExacTrac system which could be used as a reference to define the isocenter for the AlignRT. This process is called recalibration. First, the phantom was positioned by ExacTrac, and the Winston-Lutz measurements were taken of the lateral and longitudinal shifts the phantom. These shifts were small due to the better accuracy of the ExacTrac. Then the AlignRT was recalibrated, assuming the same isocenter as the ExacTrac. The phantom was then shifted arbitrarily away from the location. Using the new calibration and real-time monitoring of AlignRT, the phantom was then manually returned to the isocenter position according to AlignRT. Another Winston-Lutz test was then carried out, as shown in Table 17 confirming that the phantom was indeed repositioned well. However, when the same procedure was tried with phantom at couch angle of 90° and 270°, the AlignRT was not able to bring the phantom back to its isocenter position.

Table 1. Example of the shifts measured from repeated Winston-Lutz tests images of the Winston-Lutz pointer.

Image #	Lateral shifts (mm)	Long. shifts (mm)
1	0.02	0.21
2	0.07	0.23
3	0.06	0.29
4	0.06	0.22
5	0.05	0.3
6	-0.01	0.27
7	0.09	0.29
8	0.04	0.28
9	-0.01	0.3
10	0.01	0.28
Average	0.04	0.26
Max Dev	0.05	0.05

Table 2. Example of the shifts measured from repeated Winston-Lutz tests images of the phantom.

Image #	Lateral shifts (mm)	Long. shifts (mm)
1	-0.15	0.08
2	-0.17	0.19
3	-0.15	0.17
4	-0.13	0.16
5	-0.14	0.17
6	-0.14	0.18
7	-0.10	0.20
Average	-0.14	0.16
Std Dev	0.04	0.08

Table 3. Comparison of EPID and film.

Images taken by	Lateral shifts (mm)	Long. shifts (mm)
Film	0.25	-0.11
Film	0.26	-0.13
EPID	0.29	-0.08
EPID	0.31	-0.09
EPID	0.38	-0.10
EPID	0.31	-0.14
EPID	0.33	-0.12

Table 4. Relative shifts of the Winston-Lutz pointer measured by ExacTrac.

Orientation	Shift(mm)
VRT_{exa}^{ptr} (A/+)	-0.35
LNG_{exa}^{ptr} (S/+)	0.37
LAT_{exa}^{ptr} (L/+)	0.11

Table 5. Winston-Lutz test measurements of the Winston-Lutz pointer**.**

Gantry angle(°)	Collimator angle(°)	ΔX (mm)	ΔY (mm)	ΔTotal (mm)
0	90	0.10	-0.27	0.28
90	90	-0.17	-0.57	0.60
270	90	0.07	-0.63	0.64
0	270	-0.05	-0.45	0.46
90	270	-0.26	-0.73	0.78
270	270	0.02	-0.78	0.78

Table 6. Offset of the cone relative to the gantry isocenter.

	Gantry angles(°)	Collimator angle(°)	Offset (mm)
LAT_g^{cone} (L/+)	90 and 270	90	-0.05
	90 and 270	270	-0.12
	0	90 and 270	0.08
LNG_g^{cone}(I/+)	0	90 and 270	0.09
	90	90 and 270	0.08
	270	90 and 270	0.08

Table 7. Offset of pointer relative to gantry isocenter.

	Gantry angles(°)	Collimator angle(°)	Offset (mm)
VRT_g^{ptr} (A/+)	90 and 270	90	-0.12
	90 and 270	270	-0.14
LAT_g^{ptr} (L/+)	0	90 and 270	0.03
LNG_g^{ptr} (I/+)	0	90 and 270	-0.36
	90	90 and 270	-0.65
	270	90 and 270	-0.71

Table 8. Offsets of ExacTrac isocenter relative to gantry isocenter.

	Gantry angles(°)	Collimator angle(°)	Offset (mm)
VRT_g^{exa} (A/+)	90 and 270	90	0.23
	90 and 270	270	0.21
LAT_g^{exa}(L/+)	0	90 and 270	-0.09
LNG_g^{exa}(I/+)	0	90 and 270	0.01
	90	90 and 270	-0.28
	270	90 and 270	-0.34

Table 9. Wiston-Lutz tests results of the phantom for different gantry and collimator angles.

Gantry angle(°)	Collimator angle(°)	ΔX (mm)	ΔY (mm)	ΔTotal (mm)
0	90	0.16	-0.48	0.50
90	90	-0.39	-0.78	0.87
270	90	0.16	-0.86	0.88
90	270	-0.01	-0.64	0.64
90	270	-0.49	-0.92	1.04
270	270	-0.04	-1.05	1.05

Table 10. Cone offsets calculated from the Winston-Lutz tests of the phantom.

	Gantry angles(°)	Collimator angle(°)	Offset (mm)
LAT_g^{cone} (L/+)	90 and 270	90	-0.12
	90 and 270	270	-0.27
	0	90 and 270	0.09
LNG_g^{cone}(I/+)	0	90 and 270	0.08
	90	90 and 270	0.07
	270	90 and 270	0.10

Table 11. Offset of the BB relative to gantry calculated from Winston-Lutz measurements of the phantom.

	Gantry angles(°)	Collimator angle(°)	Offset (mm)
VRT_g^{ptr} (A/+)	90 and 270	90	-0.28
	90 and 270	270	-0.23
LAT_g^{ptr} (L/+)	0	90 and 270	0.08
LNG_g^{ptr} (I/+)	0	90 and 270	-0.56
	90	90 and 270	-0.85
	270	90 and 270	-0.96

Table 12. Offset of the "ExacTrac isocenter" to the gantry isocenter.

	Gantry angles(°)	Collimator angle(°)	Offset (mm)
VRT_g^{exa} (A/+)	90 and 270	90	-0.41
	90 and 270	270	-0.36
LAT_g^{exa} (L/+)	0	90 and 270	0.10
LNG_g^{exa} (I/+)	0	90 and 270	-0.46
	90	90 and 270	-0.75
	270	90 and 270	-0.86

Table 13. Offsets of the phantom measured by AlignRT after localization by ExacTrac.

No. of readings	ΔVRT (cm)	ΔLNG (cm)	ΔLAT (cm)	ΔLNG° (°)	ΔLAT° (°)	ΔRTN (°)
1	0.19	0.12	-0.11	0.11	0.93	-0.24
2	0.17	0.12	-0.11	0.05	0.70	0.19
3	0.16	0.13	-0.11	0.09	0.73	0.29
Average	0.17	0.12	-0.11	0.08	0.79	0.08

Table 14. Repeatability of consecutive AlignRT measurements of the same phantom.

No. of Readings	ΔVRT (cm)	ΔLNG (cm)	ΔLAT (cm)
1	0.21	0.05	0.00
2	0.21	0.03	0.00
3	0.22	0.05	0.01
4	0.21	0.03	0.00
5	0.21	0.04	0.00
6	0.21	0.04	0.00
7	0.2	0.03	0.00
8	0.23	0.04	0.00
9	0.23	0.04	0.00
10	0.22	0.04	0.00
Average (cm)	0.22	0.04	0.00
Max dev (cm)	0.01	0.01	0.01

Table 15. AlignRT measurements of the Rando phantom setup shifts for different body contour CT density cutoff values.

Cutoff values(HU)	ΔVRT (cm)	ΔLNG (cm)	ΔLAT (cm)
-350	0.09	0.12	0.01
-100	0.19	0.12	0.03
-500	-0.02	0.12	0.02
-900	-0.17	0.08	-0.08

Table 16. Testing the consistence of effect of the CT density cutoff for body contour of the phantom on the AlignRT measurement of the setup shifts.

Cutoff values(HU)	ΔVRT (cm)	ΔLNG (cm)	ΔLAT (cm)
-350	0.19	0.15	-.03
-100	0.32	0.16	-.01
-500	-0.10	0.13	-.03
-900	-0.06	0.14	-0.01

Table 17. VisionRT measurements before and after recalibration.

	Gantry angle(°)	Collimator angle(°)	Couch angle(°)	ΔX (mm)	ΔY (mm)	LAT (mm)	LNG (mm)
Before recalibration	0	90	0	0.18	0.01	-0.12	-0.11
	0	270	0	-0.41	-0.22		
After recalibration	0	90	0	0.33	-0.10	0.04	-0.25
	0	270	0	-0.25	-0.40		
	0	90	90	-1.18	0.40	-1.44	0.33
	0	270	90	-1.70	0.26		
	0	270	270	-2.22	-0.83	-1.94	-0.71
	0	90	270	-1.66	-0.58		

Chapter 5. Discussion and Conclusion

The procedure of measuring the accuracy of ExacTrac and AlignRT systems made no assumption of which system was more accurate than the other prior to setting up the phantom. However, after it was shown repeatedly that a discrepancy existed between ExacTrac and AlignRT, the experiments were refined in such a way that the relative offset of the ExacTrac to the gantry isocenter could be measured and calculated. This in turn led to the estimation of the accuracy of the AlignRT.

The Winston-Lutz measurement showed that the ExacTrac was indeed accurately calibrated, as shown by Table 8. The shifts between ExacTrac isocenter and the gantry isocenter were seen here to be very small, within 0.25mm±0.37mm, which according to published data was close to the best accuracy achievable for ExacTrac.

Since gantry sag introduces inaccuracy, the modified Winston-Lutz tests in this study were performed for gantry angles of 0°, 90°, 270° and collimator angles of 90° and 270°. The gantry angle of 180° was not included in the calculation. For vertical shift that did not use collimator angles, this would provide two sets of data to compare, namely one from 90° and another from 270° collimator angles. For longitudinal shift, three sets of data were available from the Y shift: gantry at 0°, 90°, and 270° respectively with collimator angles of 90° and

270° degrees. For lateral shift, only the X shift for collimator angles of 90° and 270° and gantry at 0°. When gantry was at 180°, the gantry suffered slight sag, but for the purpose of comparing data with the AlignRT system, it was deemed not necessary to include such an aberration because, as we have seen, the AlignRT only used one point on the top of the dot board facing the gantry at 0° angle to calibrate. Therefore, no measurements at gantry angle of 180° were included with AlignRT and it is safe to conclude that imaging with gantry at 180° did not need to be considered.

Angular shifts appeared in both ExacTrac and AlignRT readings. ExacTrac provided these as the results of its own fusion algorithm. After the phantom was positioned with ExacTrac, these shifts fell below the threshold of 0.5°. AlignRT also provided angular shifts around lateral, longitudinal, and vertical axes. Only the rotation around vertical axis, which is the couch rotation, can be manually applied. The other two rotations were, as mentioned earlier, not practical as several iterations were required. Also, since the Winston-Lutz tests were used to image a spherical object inside the phantom, rotational adjustments to the phantom should not have an impact to the position of the object. Therefore, these small rotational shifts were deemed not able to change the fact that a discrepancy existed between ExacTrac and AlignRT.

SOURCES OF DISCREPANCY

The discrepancy as measured between ExacTrac and AlignRT was significant. Notice that the translational shifts have a unit of centimeters. Table 13 indicates is that these shifts calculated from AlignRT are significantly different than those calculated from EPID measurements, which were setup by the ExacTrac system. They indicate a discrepancy of 1.5 mm, 1.2 mm, and -1.2 mm in the vertical, longitudinal, and lateral directions between AlignRT and ExacTrac systems, well beyond the range of inaccuracies shown by the ExacTrac system. It is also beyond the desired accuracy of 1 mm used by SRS/SBRT, and in the same range of error found by Peng et al.[12]

To verify that the shift as calculated by AlignRT indeed led to an incorrect position, the shifts had been applied using Varian console and then the EPID images were taken. The images clearly showed that the ball inside the phantom was well off the center of the cone beam.

There were other factors that might introduce errors. One of them was from the uncertainty of the exact location of the phantom isocenter inside the phantom, as mentioned earlier. When the phantom was scanned by the CT, the slices that made up the entire image had a separation of 1 mm between them. Treatment planning system then used these slices to build contour and assign an isocenter. For the sphere inside the phantom, the desired location of the isocenter was the center of the sphere. But since the phantom and thus the sphere inside the

phantom consisted of slices, the assigned isocenter would not necessarily be at the center of the ball, either because the center was not on one of the slices, or because the artifacts present obscured the location. On the other hand, the Winston-Lutz tests only imaged the physical sphere, and the images captured were indications of how well the sphere was positioned but not the phantom plan isocenter.

The distance between the phantom plan isocenter and the center of the sphere can be estimated by comparing the measurements of the ExacTrac isocenter from the tests with Winston-Lutz pointer and the phantom,. It turned out that the isocenter was 0.2 mm higher in the vertical direction, 0.2 mm to the left, and 0.5 mm closer to the gantry than the center of the sphere.

This distance was thus not large enough to be responsible for the discrepancy between ExacTrac and AlignRT, as both systems used planned isocenter and not the ball center to position the phantom.

Another factor that could introduce error was the contour of the surface of the phantom because AlignRT measured the position of the phantom by comparing real-time image with the CT contour. It was known that AlignRT had difficulty to detect dark surface of the Rando phantom and covering the phantom with masking tapes was a standard practice to give a lighter surface for imaging and worked well. This added a thin layer to the surface and further raised the

question if the surface had an impact to the discrepancy between AlignRT and ExacTrac.

As shown in Table 15, the AlignRT measurements for the same phantom with different cutoff values for the body contours were different. Apparently, the choice of cutoff values had an effect on the shifts calculated by AlignRT. The shift ranged from nearly 2 mm up for -100 HU to almost 2 mm down for -900 HU. That is to say, if we had a phantom that was to resemble water, then the phantom should be moved up 2 mm according to AlignRT, and if the phantom resembled thin air, then it should move down 2 mm.

The longitudinal and lateral shifts were not affected by the chosen CT density unit as the lights from the camera of the VisionRT system covered all sides except the posterior of the phantom. Therefore, only the vertical shift change was noticeable.

If the above measured values stayed consistent, then choosing a cutoff number of -500 HU could be seen as an alternative way to measure the displacement of a phantom. But when the same experiment was repeated, the results indicated that a different value could be chosen as the cutoff number (c.f. Table 16). So it remains an open question as which number should be used, and how to justify such a choice.

The region of interest (ROI) used in AlignRT measurements could be another source of errors. It was known that the size of ROI played a role in the accuracy of the results, as reported by Peng *et al*.[12]. Therefore, several ROIs had been created and tested. There were some differences between different ROIs but none of them was in the same range of the discrepancy between AlignRT and ExacTrac.

The results from Table 17 illustrated the challenges that we are still facing now with the AlignRT system, as the AlignRT were tested using a reference image acquired by AlignRT cameras instead of one from CT contour. This would have an impact on the tracking and monitoring capabilities of AlignRT in which case the comparison is not with the CT-based contour but an image taken by AlignRT itself. The sources of the discrepancy shown in Table 17 is not yet known but will be investigated.

CONCLUSION

In this study, it was shown that the EPID, in combination with the RIT software, was a suitable and fast tool for analyzing images acquired during Winston-Lutz tests.

This study also showed that the ExacTrac system had been calibrated to its best accuracy possible according to the Winston-Lutz tests.

As of the time of this study, the indication was that the AlignRT system could not consistently meet the stringent requirement of setting up a phantom to within 1 mm accuracy based *solely* on the CT contour of the phantom and its calibration using the dotted plate. The cutoff Hounsfield units used in creating the contours were shown to have an effect on the outcome of the AlignRT measurements.

FUTURE WORK

Examining AlignRT in several other aspects is considered. This will include large couch angles, lighting conditions, monitoring and tracking during the treatments, especially on real patients.

Besides AlignRT, other studies related to this thesis research can also be considered. For example, this study demonstrated that the EPID could replace films to acquire images for concentricity analysis. The techniques could be expanded to create a quick test of the alignment of the gantry, couch, and the ExacTrac system for the purpose of SRS QA when gantry angle of 180° and several couch angles are also included. Once the lateral and longitudinal shifts of the cone and the spatial positions of the Winston-Lutz pointer are known, the deviation at different gantry, collimator, and couch angles can be calculated after images are captured at those angles. Such a test will be deemed a pass if all deviations are within certain tolerance of, for example, 1 mm.

Since the radiation fields can be both circular and square for the software to resolve the concentricity, multileaf collimator (MLC) and jaws could be investigated for collimating beams instead of cones. For this thesis, only circular fields with a cone were used. A cone was attached to a cone holder which in turn was attached to the gantry. Once the cone and cone holders were fastened, they stayed very stable and did not move at all relative to the gantry. This was advantageous over using MLC or the jaws as collimation method as both MLC and jaws could move slightly depending on the angle of the gantry. Even though the cone eliminated this possibility, it is still desired to know the accuracy when MLC and jaws are used as collimators.

A study comparing the accuracy of the ExacTrac and CBCT and a study of the couch movements have already been initiated. The insight learned from this thesis research could be very useful and will pave the way for several research projects in the near future.

Bibliography

1. S. Li, “A novel 3D-video-based refixation technique for fractionated stereotactic radiotherapy,” in *AAPM Annual Meeting*, Med. Phys., **27**, 1433 (2000).

2. S. Li, D. Liu, G. Yin, P. Zhuang, and J. Geng, “Real-time 3D-surfaceguided head refixation useful for fractionated stereotactic radiotherapy,” Med. Phys. **33**, 492–503 (2006).

3. C. Bert, K. G. Metheany, K. Doppke, and G. T. Chen, “A phantom evaluation of a stereo-vision surface imaging system for radiotherapy patient setup,” Med. Phys. **32**, 2753–2762 (2005).

4. P. J. Schöffel, W. Harms, G. Sroka-Perez, W. Schlegel, and C. P. Karger, “Accuracy of a commercial optical 3D surface imaging system for realignment of patients for radiotherapy of the thorax,” Phys. Med. Biol. **52**, 3949–3963 (2007).

5. J.Y. Jin, F.F. Yin, S.E. Tenn, P.M. Medin, T.D. Solberg, “Use of the brainlab ExacTrac X-ray 6D system in image-guided radiotherapy,” Med. Dosim. **33**, 124–134 (2008).

6. D. A. Jaffray, D. G. Drake, M. Moreau, A. A. Martinez, and J. W. Wong, "A radiographic and tomographic imaging system integrated into a medical linear accelerator for localization of bone and soft-tissue targets," Int. J. Radiat. Oncol., Biol., Phys. **45**, 773–789 (1999).

7. J. Chang, K. M. Yenice, A. Narayana, and P. H. Gutin, "Accuracy and feasibility of cone-beam computed tomography for stereotactic radiosurgery setup," Med. Phys. **34**, 2077–2084 (2007).

8. L. Masi, F. Casamassima, C. Polli, C. Menichelli, I. Bonucci, and C. Cavedon, "Cone beam CT image guidance for intracranial stereotactic treatments: Comparison with a frame guided set-up," Int. J. Radiat. Oncol., Biol., Phys. **71**, 926–933 (2008).

9. M. Herman, J. Balter, D. Jaffray, K. McGee, P. Munro, S. Shalev, M. Van Herk, and J. Wong, "Clinical use of electronic portal imaging: Report of AAPM Radiation Therapy Committee Task Group 58," Med. Phys. **28**, 712–737 (2001).

10. M. Herman, "Clinical use of electronic portal imaging," Semin. Radiat. Oncol. **15**, 157–167 (2005).

11. J. A. Tanyi, P. A. Summers, C. L. McCracken, Y. Chen, L.C. Ku, M.Fuss, "Implications of a high-definition multileaf collimator (HD-MLC) on treatment planning techniques for stereotactic body radiation therapy (SBRT): a planning study," Radiat. Oncol. **4**, 22 (2009).

12. J. L. Peng, D. Kahler, J. G. Li, S. Samant, G. Yan, R. Amdur, and C. Liu, "Characterization of a real-time surface image-guided stereotactic positioning system," Med. Phys. **37**, 5421-5433 (2010).

13. L. I. Cervino, T.Pawlicki, J.D. Lawson, S.B.Jiang, "Frame-less and mask-less cranial stereotactic radiosurgery: a feasibility study," Phys. Med. Biol. **55**, 1863-1873 (2010).

14. J. Kim, J. Jin, N. Walls, T. Nurushev, B. Movsas, I. J. Chetty, S. Ryu, "Image-guided localization accuracy of stereoscopic planar and volumetric imaging methods for stereotactic radiation surgery and stereotactic body radiation therapy: a phantom study," Int. J. Radiation Oncology Biol. Phys., in press.

15. W. Lutz, K.R. Winston, N.Maleki, "A system for stereotactic radiosurgery with a linear accelerator", Int. J. Radiat. Oncol. Biol. Phys., **14**, 373 (1988)

16. K.R. Winston and W. Lutz, Linear accelerator as a neurosurgical tool for stereotactic radiosurgery, *Neurosurgery* **22** , 454–464 (1988).